

PAPER • OPEN ACCESS

In situ observation of austenite coarsening induced by massive-like transformation during solidification in Fe–C alloys

Recent citations

- [Transformation from Ferrite to Austenite during/after Solidification in Peritectic Steel Systems: an X-ray Imaging Study](#)
Hideyuki Yasuda *et al*

To cite this article: H Yasuda *et al* 2020 *IOP Conf. Ser.: Mater. Sci. Eng.* **861** 012051

View the [article online](#) for updates and enhancements.



EEG/ECOG AMPLIFIERS
& ELECTRODES
ELECTRICAL/CORTICAL
STIMULATORS
REAL-TIME PROCESSING

g.tec
gtec.at/shop
SHOP NOW

In situ observation of austenite coarsening induced by massive-like transformation during solidification in Fe–C alloys

H Yasuda¹, T Suga¹, K Ichida¹, T Narumi¹ and K Morishita^{1,2}

¹ Department of Materials Science and Engineering, Kyoto University, Sakyo, Kyoto 606-8501, Japan

² Department of Materials Science and Engineering, Kyushu University, Nishiku, Fukuoka, 819-0395 Japan

E-mail: yasuda.hideyuki.6s@kyoto-u.ac.jp

Abstract. A massive-like transformation, in which δ -ferrite massively transforms to γ -austenite in the solid state, was examined by time-resolved X-ray imaging and X-ray diffractometry on a four-dimensional-computed tomography setup. In the unidirectional solidification of a hyperperitectic steel (0.3 mass% C) at 50 $\mu\text{m/s}$, δ dendrites, fine γ grains that are produced through the massive-like transformation, and coarse γ grains grow together in the steady state. The massive-like transformation occurred commonly in Fe-based alloys with a peritectic reaction in equilibrium. Time-resolved X-ray diffraction measurements for a peritectic steel (0.18 mass% C) showed that the massive-like transformation induced strains in the γ grains. The fine γ grains coarsened and/or vanished and new γ grains formed. The induced strains were released during coarsening. The results obtained by the observations contribute to building of a physical model for γ grain coarsening.

1. Introduction

In high-temperature steel processing, it is essential to avoid coarse γ grains (referred to as γ) because the coarse grains cannot be refined in subsequent hot working [1–3]. However, abnormal γ grain growth is produced frequently in as-cast microstructures [4]. Details of γ grain coarsening was examined by an interrupted and isothermal solidification method [1]. According to the experimental results [1], γ grain suppression needed the coexistence of a second phase, such as δ -ferrite (referred to as δ) or liquid phase and only occurred in a limited temperature range below the peritectic temperature. Subsequent cooling led to coarse γ grains of as large as 5 mm in diameter. Annealing for 600 s yielded γ grains of ~ 1 mm at 1473K and 200 μm at 1673 K. The γ grain size was smaller than that observed in abnormal coarsening. Thus, abnormal coarsening after solidification is not explained simply by the grain growth in the specimen that was heated from the α -ferrite region (referred to as α). Ambiguities exist in understanding the coarsening of γ grains during or after solidification and causes difficulties to understand and to build models for predicting the microstructure formation after the transformation from ferrite (δ) to austenite (γ). It is desired to obtain experimental data which show how γ grains coarsen for building physical model.

Previous work on the coarsening of γ grains was performed by quenching unidirectionally solidifying specimens [5]. The as-cast coarse columnar γ grain structure (referred to as CCG) in hyper-peritectic steel was investigated by a rapid unidirectional solidification method [5]. In the quench structure, fine



columnar γ grains (referred to as FCG) always existed ahead of the CCG region. The FCG disappeared owing to CCG growth. This study indicates that discontinuous changes in γ grain size differed from conventional coarsening between grains.

It is difficult to analyse the microstructure evolution in Fe-based systems with phase transformations from δ to γ and from γ to α . Thus, solidification should be observed in the Fe-based alloys in situ. Two techniques exist for in situ observation, namely, X-ray imaging using synchrotron radiation X-rays and high-temperature laser-scanning confocal microscopy [6, 7]. X-ray imaging allows for internal specimen observation and for a combination of other techniques, such as X-ray diffraction (XRD) and fluorescence X-ray analysis (EDS). However, access to synchrotron radiation facilities is limited.

Solidification of Sn-, Al-, and Mg-based alloys [8–12] was observed in situ by X-ray transmission imaging (two-dimensional, 2D imaging). Later, the technique allowed for an observation of solidification in Cu-, Ni-, and Fe-based alloys above 1300 K [13–18]. Time-resolved computed tomography (three-dimension plus time, referred to as 4D-CT) has been developed and used to observe dendrite evolution in Al–Cu alloys (pink X-ray beam, rotation of 0.1 rps) [19, 20] and Al–Mg–Si–Y₂O₃ alloys [21]. 4D-CT was extended to observe a semi-solid deformation and transgranular liquation cracking in Al–Cu alloys [22, 23]. Time-interlaced model-based iterative reconstruction (TIMBIR) was developed to improve temporal resolution [24]. A filtering technique using a phase field model was proposed to improve image quality even at a relatively high temporal resolution [25]. In addition to the three-dimensional observation, 4D-CT and XRD were combined to observe the microstructure and crystallographic orientation simultaneously [25, 26].

Two-dimensional and 3D observations using X-ray imaging proved that massive-like transformation occurred in Fe–C alloys [16–18, 27–29] and Fe–Cr–Ni alloys [30]. In this transformation, δ transforms to γ in the solid state and multiple γ grains are produced. The massive-like transformation occur in preference to the peritectic reaction, in which diffusion-controlled growth of γ occurs and γ grains are crystallographically continuous along δ . Laser-scanning confocal microscopy has also shown that the δ phase massively transforms into the γ phase [7]. In the unidirectional solidification of a hyper-peritectic carbon alloy [17, 18], the massive-like transformation was selected even at a growth rate of 5 $\mu\text{m/s}$ and a coarse γ grain existed at 200 μm behind the δ dendrite tips. Therefore, the γ grain growth could be influenced by the massive-like transformation. Recently, in situ XRD analysis before and after the massive-like transformation was achieved by using a 4D-CT setup [25]. Fine γ grains were produced through the massive-like transformation and the crystallographic orientation was distributed widely.

In this study, the steady state growth of the massive-like transformation behind the δ dendritic growth in a hyper-peritectic 0.3 mass% C alloy was confirmed and grain growth of the γ grains after the massive-like transformation was examined by XRD on a 4D-CT setup.

2. Experiments

Two-dimensional imaging of the unidirectional solidification was performed for Fe – 0.3 mass% C – 0.6 mass% Mn – 0.3 mass% Si alloys (referred to as 0.3C steel) at an imaging beamline BL20B2 at SPring-8. The preliminary results were presented previously [17, 18]. The setup for the 2D observation, which was developed by the authors' group, is shown in figure 1(a). A monochromatized 28 keV X-ray was passed from the left to the right of figure 1(a). A beam monitor with a pixel size of 2.5 $\mu\text{m} \times 2.5 \mu\text{m}$ for the transmission images and a panel-type detector with a pixel size of 50 $\mu\text{m} \times 50 \mu\text{m}$ for the XRD images was used. A specimen was pulled down at 50 $\mu\text{m/s}$ under a temperature gradient of approximately 10 K/mm. Positions of the liquid- δ , the δ - γ (fine), and the γ (fine) – γ (coarse) interfaces were measured. The diffraction spots were analysed in terms of γ grain size.

XRD data for 0.18 mass% C – 0.6 mass% Mn – 0.3 mass% Si alloys (1.18C steel) on a 4D-CT setup [25, 26], as shown in figure 1(b), were obtained at beamline BL20XU of SPring-8. X-rays with an energy of 37.7 keV were used. The specimen was inserted into a sintered Al₂O₃ pipe with inner and outer diameters of 0.8 mm and 2 mm, respectively, and placed in a graphite furnace. XRD spots were observed with a flat-panel sensor with a format of 1008 \times 682 pixels and a pixel size of 100 $\mu\text{m} \times 100 \mu\text{m}$ at a

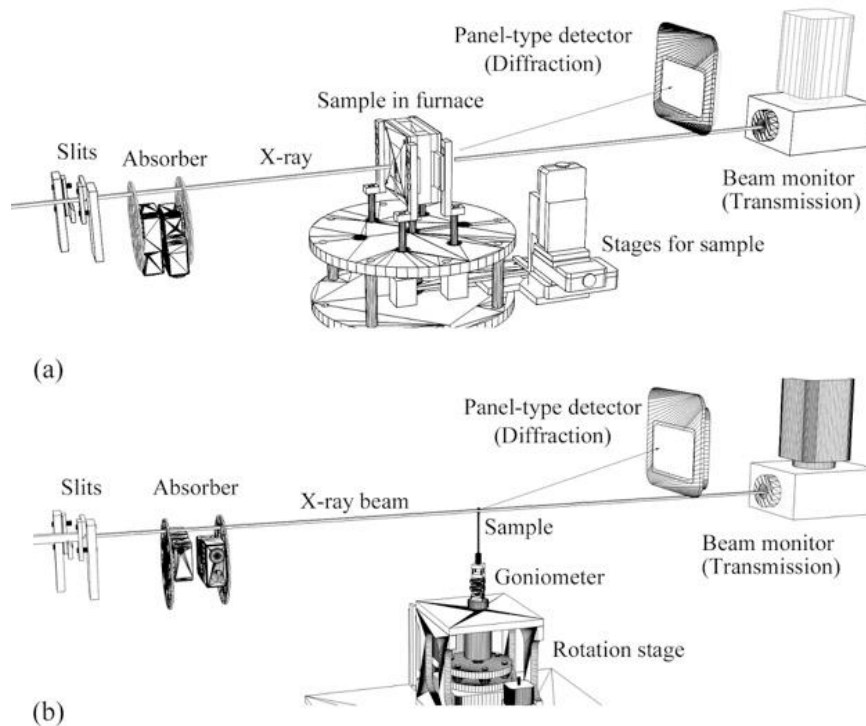


Figure 1. (a) Setup for the transmission imaging (2D observation) with X-ray diffraction and (b) setup for time-resolved tomography with X-ray diffraction. transformation.

frame rate of 30 fps. The sample was rotated at 0.25 rps and XRD spots over a 360° -rotation were obtained every 4 s. Distributions of diffracting planes were analysed.

3. Results and discussion

3.1. Unidirectional solidification

Figure 2 shows the unidirectional solidification in 0.3C steel at a pulling rate of $50 \mu\text{m/s}$ [17, 18]. Initially (0 s), liquid and δ were observed and γ exited behind the liquid- δ interface (out of the observation area) as shown in figure 2(a). The tip position of δ on the yellow axis was defined to be zero as a vertical position. As shown in figure 2(b), the solidification was completed at the δ - γ interface, which indicates that γ solidification occurred after the δ - γ transformation. Dark spots, where the Bragg condition was satisfied, were observed within the γ region at 80 s. Divergence of the X-ray beam at the beamline BL20B2 was 1.5 mrad in the vertical direction and 0.06 mrad in the horizontal direction [31]. Thus, many spots in the γ region indicated that fine γ grains with different crystallographic orientations were

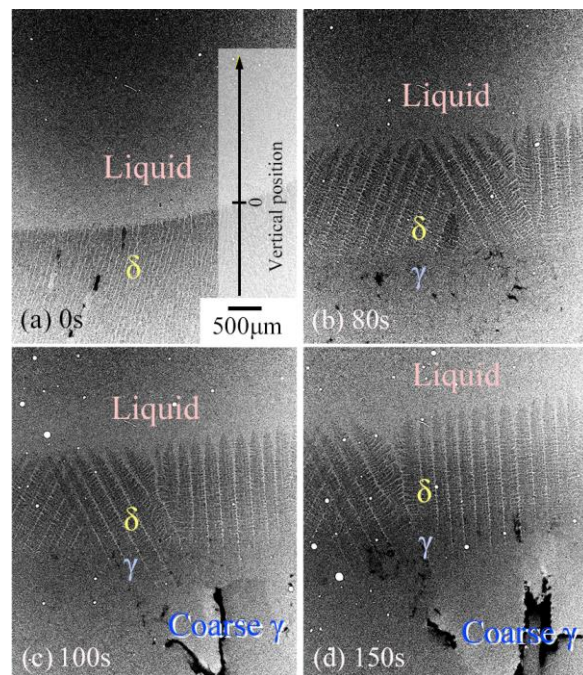


Figure 2. Unidirectional solidification of Fe-0.30C-0.6Mn-0.3Si alloy at a pulling rate of $50 \mu\text{m/s}$. (a) 0s, (b) 80s, (c) 100s and (d) 150s.

produced by the massive-like transformation. In addition to the fine γ grains behind the liquid- δ interface, a coarse γ grain, which had a front at 500 μm from the tip, appeared at 100 s, as shown in figures 2(c) and (d). The configuration of fine γ grains and a coarse γ grain is essentially the same as the microstructure from quenching during solidification [5]. The grain growth rate of the coarse γ grain is larger than the reported rate [1]. Thus, the growth rate of coarse γ grains during cooling from the melt does not agree with that observed in the specimen that was heated from the α region to the γ region.

Recently, it was reported that a massive-like transformation from δ to γ occurred at a cooling rate above 1 K/s [32]. In the massive-like transformation during the unidirectional solidification at 5 $\mu\text{m/s}$ [17, 18], the estimated cooling rate was 0.005 K/s. The observation showed that the massive-like transformation occurred even when the temperature was kept constant below the peritectic temperature [16]. The discrepancy suggests that the massive-like transformation may occur as a transient phenomenon. Thus, it is of interest to confirm the massive-like transformation during unidirectional solidification, either in the transient state or in the steady state. Figure 3 shows the position of the δ tip, the δ - γ (fine) interface, which is the front of the massive-like transformation, and the γ (fine)- γ (coarse) interface, which is the front of the crystallographically continuous γ growth, on the vertical axis in figure 2. The growth of δ into liquid and the growth of fine γ reached a steady state at 100 s. The growth of coarse γ also reached a steady state. The positions showed that the front of coarse γ did not overtake the front of fine γ . The configuration of FCG and CCG in the quenched specimen [5] is consistent with the observation result in figure 2. We conclude that the massive-like transformation is selected even at a growth rate of 5 $\mu\text{m/s}$.

Figure 4 shows a snapshot in the unidirectional solidification and an XRD image. The dark regions in the transmission images range from less than 100 μm to several 100 μm . Dark regions correspond to

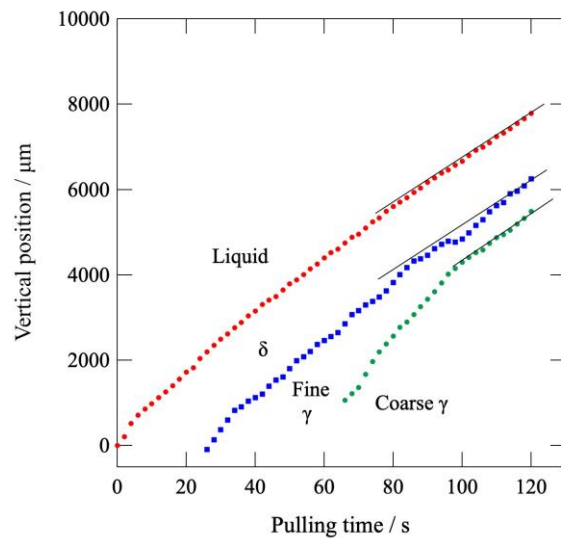


Figure 3. Positions of liquid- δ interface, δ - γ (fine) interface and γ (fine)- γ (coarse) interface during the unidirectional solidification at 50 $\mu\text{m/s}$.

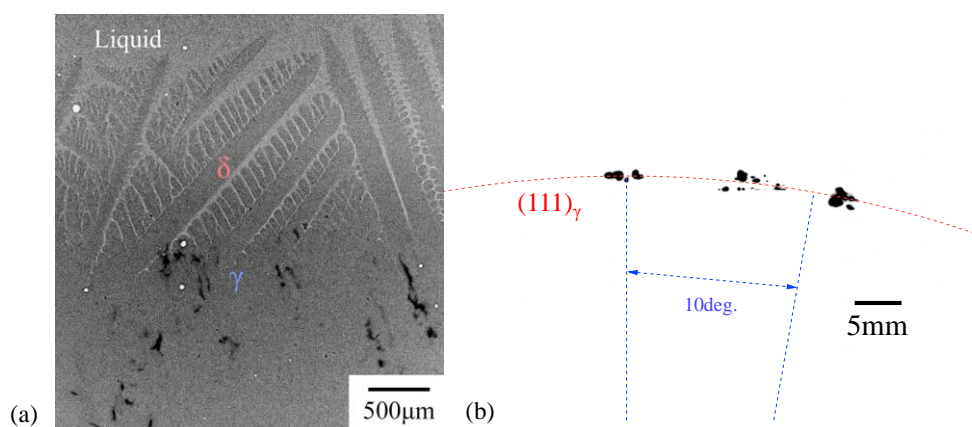


Figure 4. (a) Snapshot of the unidirectional solidification and (b) close-up view of (111) spots at the time.

the grain shape where the Bragg condition is satisfied, because the diffraction angle, 2θ , was approximately 10° . The XRD spots of the (111) plane in figure 4(b) showed that the fine γ grains were produced through the massive-like transformation. Some spots tended to segregate in a certain direction, which indicates that γ grains exist with similar crystallographic orientations and/or a large strain was induced in a single γ grain.

3.2. Coarsening of γ grains

Figure 5 shows examples of XRD images over a 3° -rotation, obtained from the panel-type detector. The rotation angles of specimen are the same. The diffraction spots varied after the massive-like transformation. As indicated by a red arrow, the XRD spots varied gradually after the massive-like transformation and some spots vanished. The change in spots indicates that a coarsening of γ grains commenced after the massive-like transformation.

Normal vectors of (111), (200), and (220) are plotted in stereo projections [33] in figure 6. The stereo projections draw the intensities of XRD spots over a 360° -rotation. Orange solid lines indicate the measurable limits at the low- and high-angle sides. Time was designated to be zero when the massive-like transformation was detected.

The spots of δ before the massive-like transformation correspond to those obtained from a single crystal, although the spots spread within 5° . As shown in figure 6(b), the crystallographic orientations of the γ grains spread widely at 0–4 s, which indicates that multiple γ grains were produced even in a single δ grain. The production of fine γ grains in single δ grains was observed in 0.45 mass% C steel and a single

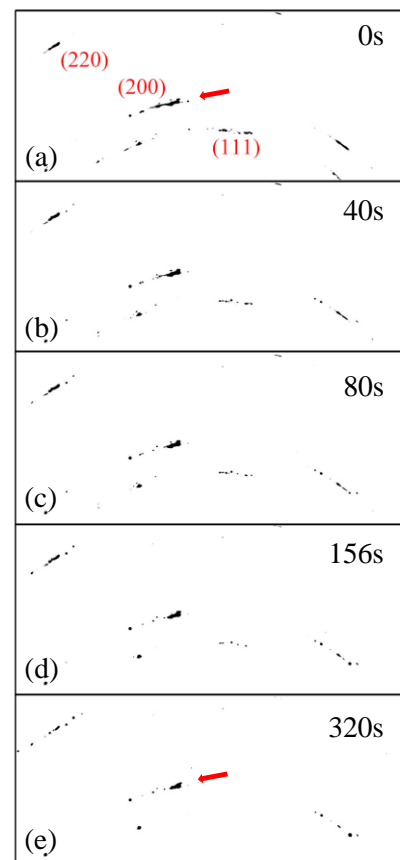


Figure 5. Diffraction spots after the massive-like transformation. Sample rotation angles are the same each other. (a) 0s, (b) 40s, (c) 80s, (d) 156s and (e) 320s.

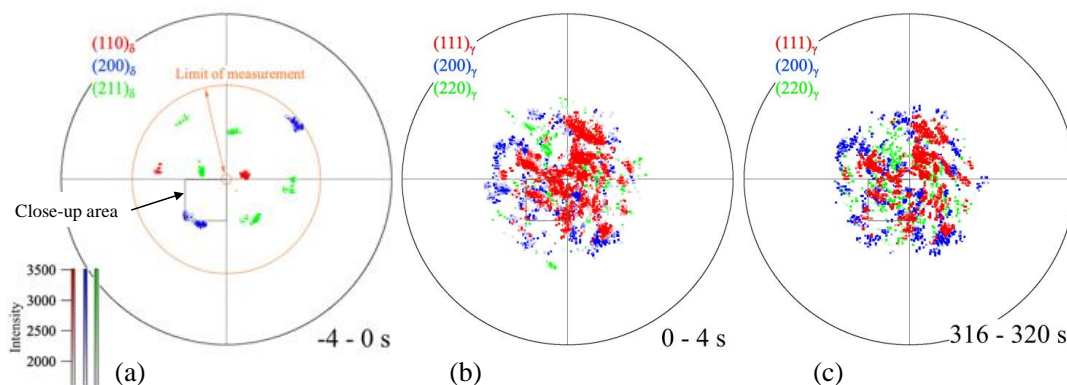


Figure 6. Crystallographic orientations. (a) δ phase before the massive-like transformation, (b) γ phase at 0–4 s after the transformation and (c) γ phase at 316–320 s.

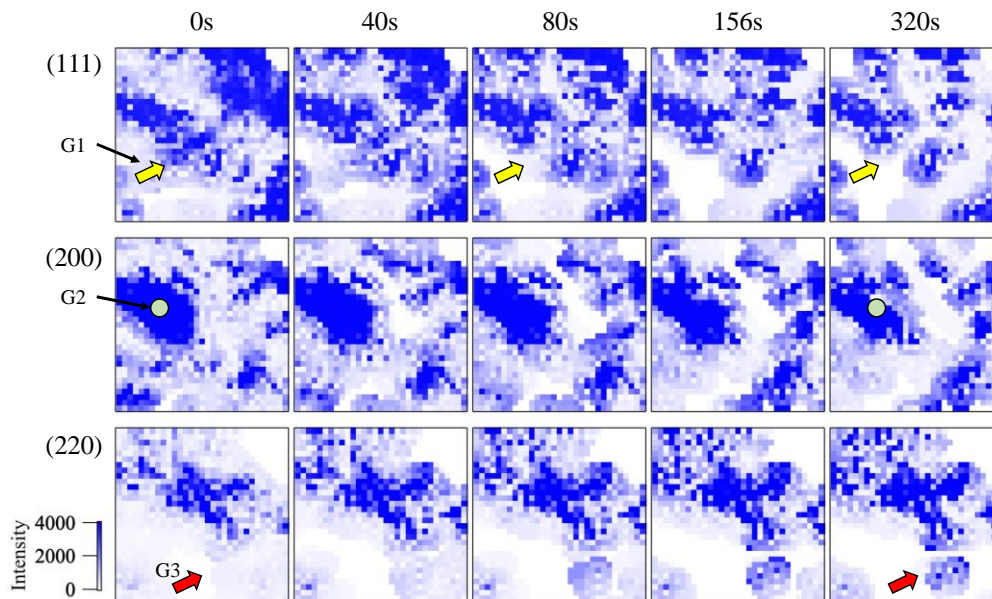


Figure 7. Close-up views of diffraction spots. The close-up area indicated in figure 6 is depicted. Yellow arrows: spots disappearing, green circles: spots sharpened and red arrows: spots newly appearing during coarsening of γ grains.

dendrite was divided into pieces owing to melting at the γ grain boundaries [16]. Thus, the observation of multiple γ grains in this study is consistent with the observation for different conditions [16]. Multiple γ grain formation in a single γ grain is a required condition for defining the massive-like transformation. Figure 6(c) shows the distribution at 316–320 s. Compared with figure 6(b), the scatter of each plane tended to decrease with an increase in time after the massive-like transformation. Some spots vanished during coarsening. It would be interesting to examine how the coarsening proceeded after the massive-like transformation.

Figure 7 shows close-up views of the stereo-projections, with an area indicated by a rectangle in figure 6(a). The distributions of (111), (200), and (222) planes are drawn separately. The “G1” intensity, which is indicated by yellow arrows in the (111) plane decreased immediately after the massive-like transformation and vanished at 320 s. Therefore, γ grains with the direction of “G1” vanished or changed their crystallographic orientation gradually during coarsening. The “G2” intensities, which are indicated by green circles, spread widely immediately after the massive-like transformation and converged gradually to a narrower region during coarsening. The gradual change in crystallographic orientation is attributed to the release of strains that are induced in a γ grain; the strains that caused a distribution of

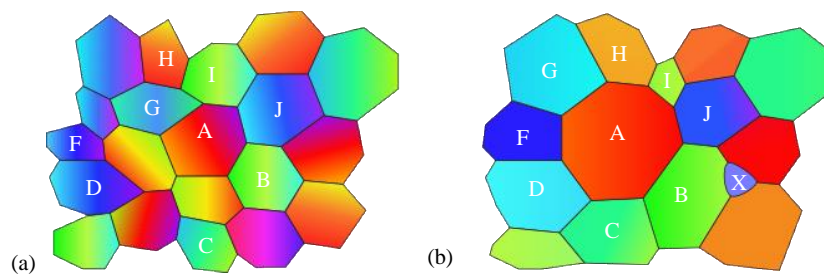


Figure 8. Schematic illustration of coarsening of γ grains after the massive-like transformation. (a) γ grains just after the massive-like transformation and (b) γ grains during coarsening. Colors in the grains correspond to crystallographic orientation.

several degrees in the crystallographic orientation were introduced in the massive-like transformation. The strains in this study are consistent with large strains that were observed by time-resolved Laue diffraction using white X-rays [28]. Although it is difficult to estimate the distribution by XRD of white X-rays, this study using a monochromatized X-ray to confirm the induced strains. The volume decreased 0.5 % by the transformation from δ to γ [18]. The volume change can induce strains within γ grains even above 1673K. “G3” is indicated by red arrows formed, which suggests that new grains were produced during coarsening. The production of new γ grains may correspond to strains within γ grain strain produced by the massive-like transformation.

Figure 8 shows schematic illustrations of γ grains immediately after the massive-like transformation and during coarsening to summarize the observation results. The fine γ grains in which strains are induced are produced through the massive-like transformation. The crystallographic orientation changes within a γ grains can reflect lattice defects in the γ grains. After the massive-like transformation, γ grains coarsened and/or vanished. The strains that were induced in the γ grains were released and this process can influence the kinetics of γ grain coarsening. The influence of the massive-like transformation modifies the coarsening kinetics in subsequent cooling after solidification and is different, compared with the kinetics [1–4].

4. Summary

The massive-like transformation in Fe–C alloys was examined by time-resolved X-ray imaging (2D observation) and XRD on a 4D-CT setup.

The observation results for the unidirectional solidification were analysed extensively. In the unidirectional solidification in 0.3C steel at 50 $\mu\text{m/s}$, δ dendrites, fine γ grains that were produced through the massive-like transformation, and coarse γ grains can grow together in the steady state. The XRD images indicated that fine γ grains formed during unidirectional solidification. Based on detailed analysis, we concluded that the massive-like transformation was selected even at low growth rates.

Changes in the crystallographic orientations of γ grains during coarsening were analysed. Strains in the γ grains were induced by the massive-like transformation. The fine γ grains coarsened and/or vanished after the massive-like transformation and new γ grains formed. The strains were released during coarsening. The massive-like transformation can modify the kinetics of γ grain coarsening.

Acknowledgments

In situ observations (2D and 3D observations) using synchrotron radiation X-rays were performed as general projects (2016B1458, 2017B1463, 2018A1380, 2019A1400) at the BL20B2 and the BL20XU of SPring-8 (JASRI), Japan. The study was initiated by “Heterogeneous Structure Control: Towards Innovative Development of Metallic Structural Materials” in the Industry–Academia Collaborative R&D Program (JST). The study was supported by a Grant-in-Aid for Scientific Research (S) (No. 17H06155). We thank Laura Kuhar, PhD, from Edanz Group (www.edanzediting.com/ac) for editing a draft of this manuscript.

References

- [1] Pottore N S, Garcia C I and DeArdo A J 1991 *Metall. Trans. A* **22** 1871
- [2] Cuddy L J and Raley J C 1983 *Metall. Trans. A* **14** 1989
- [3] Yoshida N, Kobayashi Y and Nagai K 2004 *Tetsu-to-Hagane* **90** 198
- [4] Manohar P A, Dunne D P, Chandra T and Killmore C R 1996 *ISIJ Int.* **36** 194
- [5] Tsuchiya S, Ohno M, Matsuura K and Isobe K 2011 *Acta Mater.* **59** 3334
- [6] Shibata H, Arai Y, Suzuki M and Emi T 2000 *Metall. Mater. Trans. B* **31** 981
- [7] Griesser S, Reid M, Bernhard C and Dippenaar R 2014 *Acta Mater.* **67** 335
- [8] Mathiesen R H, Arnberg L, Mo F, Weitkamp T and Snigirev A 1999 *Phys. Rev. Lett.* **83** 5062
- [9] Yasuda H, Ohnaka I, Kawasaki K, Sugiyama A, Ohmichi T, Iwane J and Umetani K 2004 *J. Cryst. Growth* **262** 645
- [10] Li B, Brody H and Kazimirov A 2004 *Phys. Rev. E* **70** 062602

- [11] Schenk T *et al.* 2005 *J. Cryst. Growth* **275** 201
- [12] Wang T, Xu J, Xiao T, Xie H, Li J, Li T and Cao Z 2010 *Phys. Rev. E* **81** 42601
- [13] Yasuda H *et al.* 2009 *Int. J. Cast Met. Res.* **22** 15
- [14] Yasuda H, Nagira T, Yoshiya M, Nakatsuka N, Sugiyama A, Uesugi K and Umetani K 2011 *ISIJ Int.* **51** 402
- [15] Kareh K M, O'Sullivan C, Nagira T, Yasuda H and Gourlay C M 2017 *Acta Mater.* **125** 187
- [16] Yasuda H, Morishita K, Nakatsuka N, Nishimura T, Yoshiya M, Sugiyama A, Uesugi K and Takeuchi A 2019 *Nat. Commun.* **10** 3183
- [17] Nishimura T, Morishita K, Yoshiya M, Nagira T and H Y 2020 *ISIJ Int.* in press (doi:10.2355/isijinternational.ISIJINT-2019-6)
- [18] Nishimura T, Morishita K, Yoshiya M, Nagira T and Yasuda H 2019 *Tetsu-To-Hagane* **105** 168
- [19] Ludwig O, Dimichiel M, Salvo L, Suéry M and Falus P 2005 *Metall. Mater. Trans. A* **36** 1515
- [20] Aagesen L K, Fife J L, Lauridsen E M and Voorhees P W 2011 *Scr. Mater.* **64** 394
- [21] Daudin R, Terzi S, Lhuissier P, Salvo L and Boller E 2015 *Mater. Des.* **87** 313
- [22] Cai B, Karagadde S, Yuan L, Marrow T J, Connolley T and Lee P D 2014 *Acta Mater.* **76** 371
- [23] Karagadde S *et al.* 2015 *Nat. Commun.* **6** 8300
- [24] Gibbs J W, Mohan K A, Gulsoy E B, Shahani A J, Xiao X, Bouman C A, De Graef M and Voorhees P W 2015 *Sci. Rep.* **5** 11824
- [25] Yasuda H, Hashimoto T, Sei N, Morishita K and Yoshiya M 2019 *IOP Conf. Ser. Mater. Sci. Eng.* **529** 012013
- [26] Nakano K, Narumi T, Morishita K and Yasuda H 2020 *Mater. Trans.* **61** in press
- [27] Yasuda H *et al.* 2011 *IOP Conf. Ser. Mater. Sci. Eng.* **27** 012084
- [28] Yasuda H *et al.* 2012 *IOP Conf. Ser. Mater. Sci. Eng.* **33** 012036
- [29] Nishimura T, Morishita K, Nagira T, Yoshiya M and Yasuda H 2015 *IOP Conf. Ser. Mater. Sci. Eng.* **84** 012062
- [30] Nishimura T, Matsubayashi R, Morishita K, Yoshiya M, Nagira T and Yasuda H 2019 *ISIJ Int.* **59** 459
- [31] Goto S *et al.* 2001 *Nucl. Instruments Methods Phys. Res. Sect. A Accel. Spectrometers, Detect. Assoc. Equip.* **467–468** 682
- [32] Liu T, Long M, Chen D, Huang Y, Yang J, Duan H, Gui L and Xu P 2020 *Metall. Mater. Trans. B* **51** 338
- [33] Yoshiya M, Nakajima K, Watanabe M, Ueshima N, Nagira T and Yasuda H 2015 *Mater. Trans.* **56** 1461